Lacunar-canalicular network in femoral cortical bone is reduced in aged women and is predominantly due to a loss of canalicular porosity

Bone Reports 7 (2017) 9–16

Contents lists available at ScienceDirect

Bone Reports

journal homepage: www.elsevier.com/locate/bonr

Lacunar-canalicular network in femoral cortical bone is reduced in aged women and is predominantly due to a loss of canalicular porosity

A.M. Ashique [a], L.S. Hart [a], C.D.L. Thomas [b], J.G. Clement [b], P. Pivonka [c,d], Y. Carter [e], D.D. Mousseau [f], D.M.L. Cooper [a,*]

[a] Department of Anatomy & Cell Biology, University of Saskatchewan, Saskatoon, SK, Canada
[b] Melbourne Dental School, University of Melbourne, Melbourne, VIC, Australia
[c] St. Vincent's Department of Surgery, University of Melbourne, Melbourne, VIC, Australia
[d] School of Chemistry, Physics and Mechanical Engineering, Queensland University of Technology, Brisbane, QLD, Australia
[e] Department of Radiology, University of Massachusetts Medical School, Worcester, MA, USA
[f] Department of Psychiatry, University of Saskatchewan, Saskatoon, SK, Canada

ARTICLE INFO

Article history:
Received 16 February 2017
Received in revised form 29 May 2017
Accepted 27 June 2017
Available online 28 June 2017

Keywords:
Bone
Lacunae
Canaliculi
Human aging
Confocal laser scanning microscopy

ABSTRACT

The lacunar-canalicular network (LCN) of bone contains osteocytes and their dendritic extensions, which allow for intercellular communication, and are believed to serve as the mechanosensors that coordinate the processes of bone modeling and remodeling. Imbalances in remodeling, for example, are linked to bone disease, including fragility associated with aging. We have reported that there is a reduction in scale for one component of the LCN, osteocyte lacunar volume, across the human lifespan in females. In the present study, we explore the hypothesis that canalicular porosity also declines with age. To visualize the LCN and to determine how its components are altered with aging, we examined samples from young (age: 20–23 y; $n = 5$) and aged (age: 70–86 y; $n = 6$) healthy women donors utilizing a fluorescent labelling technique in combination with confocal laser scanning microscopy. A large cross-sectional area of cortical bone spanning the endosteal to periosteal surfaces from the anterior proximal femoral shaft was examined in order to account for potential trans-cortical variation in the LCN. Overall, we found that LCN areal fraction was reduced by 40.6% in the samples from aged women. This reduction was due, in part, to a reduction in lacunar density (21.4% decline in lacunae number per given area of bone), but much more so due to a 44.6% decline in canalicular areal fraction. While the areal fraction of larger vascular canals was higher in endosteal vs. periosteal regions for both age groups, no regional differences were observed in the areal fractions of the LCN and its components for either age group. Our data indicate that the LCN is diminished in aged women, and is largely due to a decline in the canalicular areal fraction, and that, unlike vascular canal porosity, this diminished LCN is uniform across the cortex.

1. Introduction

Bone microarchitecture is highly elaborate, as it is organized on a number of hierarchical levels (Weiner and Wagner, 1998). This includes the interconnected vascular canal network and smaller-scale lacunar-canalicular network (LCN); these two interconnected networks provide conduits throughout the mineralized bone matrix for movement of blood and interstitial fluid, respectively. The adequate supply of nutrients, disposal of waste products, and exchange of regulatory signals through the LCN is essential for the viability and function of osteocytes contained within their lacunae (Bonewald, 2007; Kogianni and Noble, 2007). The function of osteocytes is to regulate bone metabolism, mechanosensation/mechanotransduction, and adaptation/bone remodeling processes (Jilka and O'Brien, 2016). The LCN comprises a significant part of the bone volume within the skeleton (~4.2% (Cowin, 1999)) and its communication network has been postulated to be of the same magnitude of complexity as the neural network in the brain (Buenzli and Sims, 2015). A significant reduction in LCN surface area could impair mineral mobilization and/or the mechanotransductive function of the osteocyte syncytium due to "metabolic starvation", which, in turn, would lead to increased turnover of the matrix (Currey, 1964). Reduced interconnectivity could also hinder osteocyte communication and ultimately, bone remodeling. Since some bone diseases are commonly associated with aging, a better understanding of how age influences the LCN will provide insight into the relation between the LCN, bone health and aging.

Osteocytes reside within lacunar pores, which are broadly distributed throughout the bone matrix. It is from within these lacunae that osteocytes regulate the dynamic processes of bone, including modeling and remodeling. The shape and size of lacunae vary significantly within and

* Corresponding author.
E-mail address: dml.cooper@usask.ca (D.M.L. Cooper).

http://dx.doi.org/10.1016/j.bonr.2017.06.002

between species. In rodents and humans, they range from larger elongated ovoid to smaller spherical spaces (Hirose et al., 2007; Okada et al., 2002; van Hove et al., 2009) and this variation is dependent on anatomical location (Carter et al., 2013a; Carter et al., 2013b; Vatsa et al., 2008). There remains some contention as to whether lacunae size changes with age. Our own work has revealed that lacunar volume decreases in women, but not in men (Carter et al., 2013a), although another group observed an increase in women (Atkinson and Hallsworth, 1983). A decline in osteocyte lacunar density with age was found in human trabecular (Mori et al., 1997; Mullender et al., 1996; Qiu et al., 2002) and cortical bone (Carter et al., 2013a; Carter et al., 2013b; Vashishth et al., 2005). The relation between lacunar density and bone disease is currently unclear as both an increase (Mullender et al., 1996; Vashishth et al., 2005; Soicher et al., 2011) and a decrease (Mori et al., 1997; Mullender et al., 2005; Qiu et al., 2003) in lacunar density has been observed in osteoporotic individuals.

Osteocytes communicate with each other and with cells at the bone's internal and external surfaces (such as bone marrow, bone-lining cells, and osteoblasts) via dendritic cellular processes that form an expansive 3-dimensional (3D) network of tortuous canals, called canaliculi (Kamioka et al., 2001; Palumbo et al., 1990; Shapiro et al., 1995). The orientation of the canaliculi is quite random in juvenile rodents, but becomes more organized (oriented perpendicular to surfaces) and extensive with maturation in adults (Hirose et al., 2007; Okada et al., 2002). Yet, this elaborate organization ultimately diminishes in aged rodents (Okada et al., 2002) and is likely the cause of the reduced fluid flow in bone (due to reduced permeability) observed in 7 month old mice, compared to mice at 2 months of age (Rodriguez-Florez et al., 2014). Reduced LCN interconnectivity has also been reported in osteoporotic individuals (Knothe Tate et al., 2002), as has increased heterogeneity of the network (Knothe Tate et al., 2002; Knothe Tate et al., 2004). Milovanovic and colleagues used an acid etch/SEM technique to analyze the mid-cortical region of the femur and showed that there are 30% fewer canaliculi directly arising from lacunae that reside within osteons and fewer canaliculi crossed the cement line in an aged mixed population of men and women (Milovanovic et al., 2013). As a result, lacunar-canalicular connections were reduced within osteons, but the interstitial lacunar-canalicular connections were not investigated (Milovanovic et al., 2013).

We previously reported a 30% decline in osteocyte lacunar size in women >50 years compared to women <50 years of age using synchrotron radiation micro-computed tomography (μCT; Carter et al., 2013a) at a resolution that was unable to resolve canaliculi. Here we explore the hypothesis that this reduction in lacunar size is accompanied with, and possibly related to, a reduction in canaliculi arising from osteocytes since a large number of protruding canaliculi would broaden the osteocytes outer surface and potentially increase lacunar volume. To test this hypothesis, we utilized a fluorescence labelling procedure and a higher resolution imaging technique, *i.e.* confocal laser scanning microscopy (Ciani et al., 2009), to compare cortical bone from the femoral diaphysis of young and aged women with no known history of bone disease. Our primary objective was a broad analysis of the LCN porosity as a whole, and separated into its lacunar and canalicular components, spanning the entire cortex and including osteonal and interstitial bone. Our secondary objective was to explore potential regional variations in these parameters across the radial span of the anterior cortex.

2. Materials & methods

2.1. Specimens

Human femoral bone specimens were obtained from the Melbourne Femur Collection, which was created in partnership with the Victorian Institute of Forensic Medicine (VIFM; Australia) between 1990 and 2005 and is maintained at the Melbourne Dental School (University of Melbourne, Australia). Specimens were harvested from individuals who had died suddenly and unexpectedly, with no apparent medical condition and who did not have any known history of bone-related pharmacotherapeutic usage (Clement, 2005). Specimens were manually cleaned of external soft-tissue, fixed in 70% ethanol and then desiccated for subsequent storage and transport, a commonly utilized approach for synchrotron μCT- and phase-contrast nano-CT-based imaging of bone (Carter et al., 2013a; Carter et al., 2013b; Carter et al., 2014; Varga et al., 2015; Hesse et al., 2015). This study was conducted with ethics approval from the VIFM (EC26/2000), the University of Melbourne (HREC 980139), and the University of Saskatchewan (Bio# 08-46). We utilized transverse bone sections ($n = 11$) from the anterior region of the proximal femoral shaft that were previously mounted onto glass slides for another histological study (Hennig et al., 2015). The samples also represent a subset from those included in our previous synchrotron-based study where lacunar size was found to change with age (Carter et al., 2013a). The current study was designed to compare bone specimens from young adult women (20–23 years of age; $N = 5$) and from aged women (70–86 years of age; $N = 6$; see Supplemental Table S1 for donor information summary).

2.2. Fluorescein isothiocyanate (FITC) staining

Unstained sections (150 μm) were cut from 5 mm blocks of the anterior cortical region of the human femoral midshaft (see Fig. 1 in (Carter et al., 2013b)). These were hand-lapped to 50 μm with 2000 Grit 3M sandpaper, ultrasonically cleaned, and then mounted onto glass slides (Hennig et al., 2015). For the current study, these undecalcified and unstained sections were gently dislodged from slides by soaking in xylene for 3 days. Washing with absolute ethanol thrice for 5 min removed all traces of xylene from bone before proceeding to staining with FITC (Sigma Cat#F7250), which was used to visualize the interstitial bone space. FITC was chosen since, in our hands and from images in the literature (Ciani et al., 2009; Sharma et al., 2012), FITC staining of LCN was of much higher quality than LCN images where basic fuchsin or calcein staining was done. All FITC preparation and staining procedures were performed with minimum exposure to light (Ciani et al., 2009). A 1% FITC solution was made in absolute ethanol by shaking on a rotator for 1 h at medium speed and vortexing briefly every 15–20 min. All undissolved particulate was removed by filtration through a 0.22 μm filter. Bone sections were stained in 1% FITC at room temperature for 4 h with gentle rocking and subsequently washed 3–4 times with absolute ethanol for 15–20 min per wash. The bone sections were air-dried and then mounted with coverslips onto glass slides (Fisherbrand Superfrost Plus, Cat#12-550-15) using ProLong Diamond Antifade (Life Technologies, Cat#P36970) to preserve the fluorescence. Edges of the coverslips were sealed with nail polish and slides were preserved in a light-tight container at −20 °C.

2.3. Confocal laser scanning microscopy

Slides were brought to room temperature prior to imaging. Imaging was performed on a FluoView™ FV1000 confocal laser scanning microscope (Olympus, Japan) using oil immersion (60× lens) and the following settings: 1.4 numerical aperture, pinhole set at 1 Airy unit, wavelength excitation of 488 nm, and laser intensity set to 7.0%. The sensitivity of the detector adjustment (HV), gain and offset were optimized for each sample. Images were taken at a resolution of 1600 × 1600 pixels with a pixel resolution of approximately 0.132 μm/pixel × 0.132 μm/pixel, and a 211 μm × 211 μm field of view. The focal depth was 0.44 μm.

2.4. Image montages

The LCN in bone is inherently heterogeneous (Knothe Tate et al., 2002; Knothe Tate et al., 2004). Therefore, in order to obtain an accurate representation of LCN microarchitecture and to minimize the possibility of error associated with sampling bias, we chose to implement a two-dimensional (2D) analysis approach which would allow the assessment of the entire anterior femoral cortex from the endosteal to periosteal surfaces. The sheer size of the bone area to be investigated precluded using a three-dimensional volumetric approach, which is better suited for smaller regions of interest and therefore subject to sampling bias. The 2D plane that was chosen to be imaged was 8–10 μm below the bone surface, which was deep enough to ensure that fluorescent glare from the FITC on the edges of the bone section was eliminated along the entire large plane of section. Multiple adjacent images with overlapping edges were digitally stitched together to generate large montages using the Stitching plugin and Grid/Collection Stitching option in the *ImageJ* software platform (version 1.50i; rsbweb.nih.gov/ij/) (Preibisch et al., 2009). The width of the montages of all specimens were kept relatively constant (average width = 10,383 pixels or 1.37 mm, 7 images), but differed in their periosteal to endosteal depth (average depth = 32,298 pixels or 4.26 mm, 17 to 44 images) due to variation in cortical thickness (Table 1). Individual montages ranged from 119 to 308 images (Fig. 1A,B). The montages were then cropped such that they extended to the edges of the endosteal and periosteal surfaces (Fig. 1A,B). The cropped images were used for all subsequent analyses.

2.5. Image processing

In order to calculate the area of bone occupied by the LCN, it was necessary to segment its components – the lacunae and the canaliculi – as well as larger vascular canals (consisting of Haversian canals, non-Haversian canals and resorption spaces) and any artifacts (Fig. 1C,D). In order to do this, images were processed using *ImageJ* software. Artifacts, which were identified and removed from analysis, predominantly consisted of microcracks, but also, to a much lesser extent, included minor staining anomalies. A minimum filter (radius 10 pixels) and Otsu Auto Thresholding was used to extract vascular canals. Otsu's threshold clustering algorithm is used to automatically perform clustering-based image thresholding that minimizes the intra-class variance, defined as a weighted sum of variances of the two classes (Otsu, 1979) where, in this case, the two classes represented the background (bone) and the vascular pores. A median filter (radius 2 pixels) and Auto Local Thresholding (mean radius = 15 pixels; parameters 1 and 2 = 0) was used to extract both artifacts and lacunae (Fig. 1E,F). These thresholding parameters were selected such that the resulting binarized images closely resembled the raw confocal data (Fig. G,H). This segmentation procedure resulted in three distinct masks: i) a canal; ii) an artifacts; and, iii) a lacunae mask (Fig. 1E,F). Although segmentation conditions were optimized, the segmentations were prone to some error due to the sheer size of, and enormous structural variability within, the large montages. In order to obtain precise vascular canal, artifact, and lacunae masks, careful inspection and manual manipulation of the segmentation masks was needed. Approximately 120,000 regions of interest that were generated in the segmentation procedure were inspected for accuracy. The entire image was then carefully scanned to identify vascular canals, artifacts, or lacunae that were missed during segmentation and drawn in manually for each mask. These criteria were standardized and applied equally to all specimens.

The outlines of the non-canalicular porosity were then utilized as masks to aid in segmenting the canalicular area. The raw montages were median filtered (radius = 4 pixels) to suppress noise and the Auto Local Mean Threshold (radius = 50 pixels; parameter 1 = −25; parameter 2 = 0) of *ImageJ* was used to convert all fluorescence in the images into a binary image. The canaliculi were isolated by the removal of the artifact, vascular canal and lacunar masks. The artifact mask was expanded by 5 pixels to ensure all related fluorescent signal was removed. The LCN and canalicular percentages were calculated using the following formulae:

$$\text{LCN Area}\% = (\text{LCN Area}/(\text{Total Bone Area} - (\text{Vascular Canal Area} + \text{Artifacts Area}))) * 100$$

$$\text{Canalicular Area}\% = (\text{Canalicular Area}/(\text{Total Bone Area} - (\text{Vascular Canal Area} + \text{Artifacts Area}))) * 100$$

where Total Bone Area (mm^2) is the area comprised of the cropped endosteal to periosteal swath of cortical femur bone, Vascular Canal Area (mm^2) is the sum of all areas occupied by individual vascular canals within the Total Bone Area, Artifacts Area is the sum of all areas occupied by artifacts within the Total Bone Area, and LCN and Canalicular Area are the sum of all areas occupied by the LCN (lacunae and canaliculi) or the canaliculi within the Total Bone Area, respectively. Vascular Canal, lacunar, and canalicular porosities represent the areal fraction of bone area occupied by vascular porosity, lacunae, and canaliculi, respectively. Average lacunae size was calculated as the average cross-sectional area of each lacuna in the imaging plane. All of these parameters were assessed for the entire region of interest, spanning the cortex. Further, these parameters were assessed within periosteal, mid-cortical and endosteal regions, created by evenly dividing up the span of the cortex.

Since alterations in thresholding conditions can impact the results, we performed a sensitivity study. Briefly, we altered the thresholding parameters such that the resulting images, compared to the optically 'ideal' parameters noted above, were visually either less bright (missing structures) or more bright (overestimating the area of the LCN and canaliculi). We found that the resulting change in LCN and canaliculi percentages were minor (Supplemental Table S2). These modest fluctuations did not affect the outcomes of the study and indicated that our segmentation procedures generated robust and stable results.

2.6. Statistical analysis

Statistical analysis was conducted using SPSS V23 (IBM Analytics, Chicago, IL, USA). When comparing mean values across the whole cortex, differences between young and aged females were evaluated by Student's *t*-test for normally distributed data ($p < 0.05$ was considered significant). Data are presented as mean +/− standard deviation of the mean (SD). For the regional analysis, a repeated measures ANOVA was utilized with bone region as a within-subjects factor and age group as a between-subjects factor. Kolmogorov-Smirnov (KS) tests were used to examine the distribution of all variables and Mauchly's test was used to examine the assumption of sphericity for the repeated measures ANOVA.

3. Results

For the analysis of the mean values across the whole cortex, KS tests revealed that the distributions of all measures did not deviate from the normal distribution. In the samples from the aged women, the vascular canal porosity was increased 3.2-fold compared to samples from the young women ($p = 0.039$; Table 1). Despite this, the mean endosteal to periosteal depth was very similar (Table 1; young = 3.91 mm vs aged = 3.77 mm; $p = 0.79$). We found that the LCN comprised ~17.6% of the bone area in young women (Fig. 2A; Table 1). In aged women, however, the LCN comprised 10.5% of the bone area, which is a 40.6% reduction from that observed in younger women ($p = 0.001$; Fig. 2A; Table 1, Table S2). Lacunar porosity was not different between the two age groups ($p = 0.14$; Fig. 2B; Table 1). Similarly, the average lacunar cross-sectional size was unchanged (Fig. 2C; Table 1) and the distribution of the different sizes of lacunae were very similar in both age groups (Fig. 2D). Lacunar density was reduced by 21.4% ($p = 0.049$; Fig. 2E; Table 1). The canaliculi were found to make up 75% and 81% of the LCN area for the young and aged groups, respectively. In young women, canalicular porosity was 14.3% of the 2D bone area, while in aged women it was 7.9%, a 44.6% reduction ($p = 0.001$; Fig. 2F; Table 1, Table S2).

The cortex was then divided into equal thirds – periosteal, mid-cortex, and endosteal regions – in order to perform regional analysis across the cortex. This regional analysis, employing repeated measures ANOVA, revealed that differences in bone regions was only significant for vascular canal porosity in young women, with the periosteal measure being significantly different from both the mid-cortical ($p = 0.002$) and endosteal ($p = 0.026$) measures (Fig. 2G). While the assumption of sphericity was violated (Mauchly's test) for this measure in the young women, the significance of the result for the ANOVA was unaltered after correction for this violation (e.g. Greenhouse-Geisser, Huynh-Feldt). All other measures (LCN porosity (Fig. 2H), lacunar porosity (Fig. S1A), canalicular porosity (Fig. S1B), and lacunar density (Fig. S1C)) for both the young and the aged groups did not significantly vary by region with the caveat that lacunar area in the midcortical and endosteal regions were not normally distributed (KS test).

4. Discussion

A combination of fluorescent labelling and confocal laser scanning microscopy was used to quantitate the LCN porosity in bone specimens from young and aged women. Our results revealed a significant reduction in the LCN in aged women and that this reduction is primarily due to a significant loss in canalicular porosity. Milovanovic and colleagues reported a 30% reduction in the number of canaliculi arising from osteocyte lacunae as a consequence of aging in humans; however, it is unclear from the study how many individuals were male or female (Milovanovic et al., 2013). This is of particular importance since it is known that there is a sex-dependent influence on age-related bone fragility (Seeman, 2002). The reduction in LCN in aged women that we have shown raises questions as to whether this decline is gradual over the lifespan or whether there is a greater decline after menopause. For example, osteocyte density has been reported to be reduced due to menopause in human cancellous bone (Qiu et al., 2002), which would suggest that our observations might apply strictly to women. In the femoral head, however, osteocyte lacunar density has been reported to be unchanged in women until age 70, but falls steeply thereafter (Mori et al., 1997), which argues that our results (based on young and aged cohorts) might reflect a precipitous event rather than one that progresses over the lifespan.

The decline of the scale of the LCN in advanced age could have significant functional consequences. The LCN hosts the largest number of bone cells, osteocytes, which have been associated with bone's ability to sense and adapt to changes in the mechanical loading environment and regulate the bone remodeling process. A reduced LCN in the aged population may hamper nutrient transport/oxygen supply (Cowin, 2002) and alter pressure in the lacunae pore space (Scheiner et al., 2016), thereby impacting mechanosensing and/or mechanotransduction. The loss of nutrients may further exacerbate the loss of osteocyte syncytium connectivity with the death of osteocytes resulting in an increase in hypermineralized lacunae that is observed in aged men and women (Busse et al., 2010).

Measurement of the LCN porosity does not necessarily directly reflect the osteocyte cellular network itself since osteocytes can undergo apoptosis (Noble and Reeve, 2000). Lacunar occupancy has been reported to be 90.9–93% in trabecular bone (Qiu et al., 2006), while in deeper bone from aged individuals the degree to which lacunae are occupied can drop substantially, *i.e.* to 77.1% (Qiu et al., 2006), a feature that may be related to cell death. Canalicular occupancy is not yet known, but simply counting the canaliculi clearly provides an upper limit for the potential number of viable dendritic processes in bone. The direct imaging of osteocyte dendrites will provide the greatest insights into osteocyte connectivity, as well as canalicular occupancy, and the possibility of assessing the relation between osteocyte-dendritic cell death with canalicular removal.

A limitation of our study is the over-estimation of the bone porosity (as a percent of area) due to imaging of a fluorescent signal. The latter may be associated with leaching beyond the outer boundaries of canaliculi and lacunae (Kameo et al., 2010; Currey and Shahar, 2013) and partial volume effects resulting from the resolution limits of the confocal laser scanning microscope, which was in the 0.132 μm range for our study, whereas the canaliculi diameter is estimated to be 0.1–1.0 μm (Currey and Shahar, 2013; Benalla et al., 2014). We found that the LCN comprised ~17.6% of the bone cross-sectional area in young adults. Several approaches have been used to estimate LCN porosity, resulting in a range of values: 2.8–3.3% (synchrotron radiation phase-contrast nano-CT and Synchrotron μCT (Hesse et al., 2015; Hesse et al., 2014a; Hesse et al., 2014b)), 4.5% (μCT; (Benalla et al., 2014)); 3.5–5% (poroelastic analysis (Cowin, 1999; Gardinier et al., 2010)); 12% (Theoretical estimation based on capillary and spherical-shell models (Goulet et al., 2009)); 13.5%, 19% and 23% (using a confocal laser scanning microscopy approach that is similar to the one used in our study (Ciani et al., 2009; Sharma et al., 2012; Kameo et al., 2010)). The most probable value for LCN porosity is likely <5% since, among the techniques used, the synchrotron radiation phase-contrast nano-CT-based approaches have the highest resolution capabilities. Similarly, our lacunar porosity of 3.2% in young women was 2–3× higher than that reported in the

Table 1
Average morphological parameters of femoral cortical bone from young and aged women.

	N	Age range	Vascular canal porosity (% ± SD)	Endosteal to periosteal depth (cropped; mm ± SD)	Avg bone area (cropped; mm^2 ± SD)	LCN area (% ± SD)	Lacunar area (% ± SD)	Avg lacunae size (μm^2 ± SD)	Lacunae #/mm^2 ± SD	Canalicular area (% ± SD)
Young	5	20–23	4.8 ± 0.5	3.27 ± 0.83	4.75 ± 1.26	17.6 ± 2.9	3.2 ± 1.0	45.6 ± 8.7	695 ± 79	14.3 ± 1.9
Aged	6	70–86	15.4 ± 9.8	3.19 ± 0.92	3.99 ± 1.14	10.5 ± 2.4	2.5 ± 0.5	46.4 ± 9.3	546 ± 126	7.9 ± 2.0
% change w/age			323			−40.6	−22.8	1.7	−21.4	−44.6
$p =$			0.039			0.001	0.14	0.88	0.049	0.001

literature: 1.3% (Synchrotron μCT: Schneider et al., 2010); 1.5% (Synchrotron μCT: Tommasini et al., 2012); 1.24% (Synchrotron μCT: Carter et al., 2013b); 1.5% (μCT: Palacio-Mancheno et al., 2014); and 1.7% (μCT: Benalla et al., 2014). With this limitation in mind, we focused on the differences between young and aged women where overestimation of fluorescence would be applied equally, instead of emphasizing the absolute porosity in either young and/or aged women. We predicted that using thresholding parameters that overestimate porosities would reduce the differences between samples and, thus, underestimate differences between the age groups, which is precisely what we observed, although significant differences remained (35.1%; see Supplemental Table S2). Applying more aggressive thresholding parameters that generate images with reduced LCN scale may better approximate 'true' porosity levels, but this approach tends to exclude canaliculi that are readily evident by gross visual examination of the raw confocal images. This also increased the differences between the age groups in LCN porosity (43.0%; Supplemental Table S2). Due to the stability of the results in the face of altered thresholds, we are confident that our finding of age-related differences is robust and the range of our values is similar to that presented using this general approach.

The original impetus for this study stemmed from the previous finding by Carter and colleagues that lacunar volume declines in women over the human lifespan (Carter et al., 2013a). The approach we utilized to make this measure (synchrotron μCT at 1.4 μm voxel size) was not capable of resolving canaliculi and we hypothesized that loss of canaliculi may be associated with, and possibly contributing to, this change in lacunar volume since the large number of exiting canaliculi would augment lacunar dimensions as detected by lower resolution imaging with associated partial volume effects (Sharma et al., 2012). Unexpectedly, while our current results reveal that a decline in the LCN occurs with age in women, we did not replicate our earlier finding of declining osteocyte lacunar size. Numerous factors may have contributed to this. Carter and colleagues (Carter et al., 2013a) assessed lacunar volume in 3D where lacunae can be conceptualized as ellipsoids, whereas we examined sections where the lacunar cross-sections can be conceptualized as ellipses. This is an important distinction because a small change in the dimensions of the lacunae in 3D leads to larger changes in volume than cross-sectional area. Further, in human bone lacunae are primarily oriented longitudinally and the findings of Carter and colleagues were that the longitudinal axis saw the largest (absolute) change in size with age. In the current 2D study, we quantified lacunar area from sections perpendicular to the lacunar long axis and thus this largest change in size would not be detectable. Moreover, each lacunae detected was sectioned at a random position along its long axis, contributing further variance to the area measurement. Finally, the borders of lacunae are less distinct when canaliculi are resolved, creating yet another source of variation. We believe this collection of factors explains why we found no correlation between our current 2D lacunar areas and the 3D volumes we reported previously (Carter et al., 2013a). Additional - and more detailed - 3D analysis is required to more directly answer the question of whether or not canalicular number, and specifically the proportion of canaliculi arising directly from lacunar surfaces, contribute to lacunar size when employing lower resolution techniques and, thus, play a role in a decline in lacunar volume with age.

A second discrepancy with Carter and colleagues (Carter et al., 2013a) was that the current study found a decline in lacunar density in aged women, as assessed in an areal manner (lacunae/mm^2), whereas Carter and colleagues (Carter et al., 2013a) found no change when assessing 3D volumetric lacunar density (lacunae/mm^3). That said, our previous report (Carter et al., 2013a) did find a downward trend with age and the 3D results do correlate with our current 2D results ($r = 0.797$, $p < 0.01$). The significant difference with age for our current study is likely linked to the reduced 3D lacunar size in the aged group. The probability of lacunae being observed in section is related to their size. Smaller lacunae with more space between them in the z-plane are less likely to intersect a cross-section – particularly a very thin z-

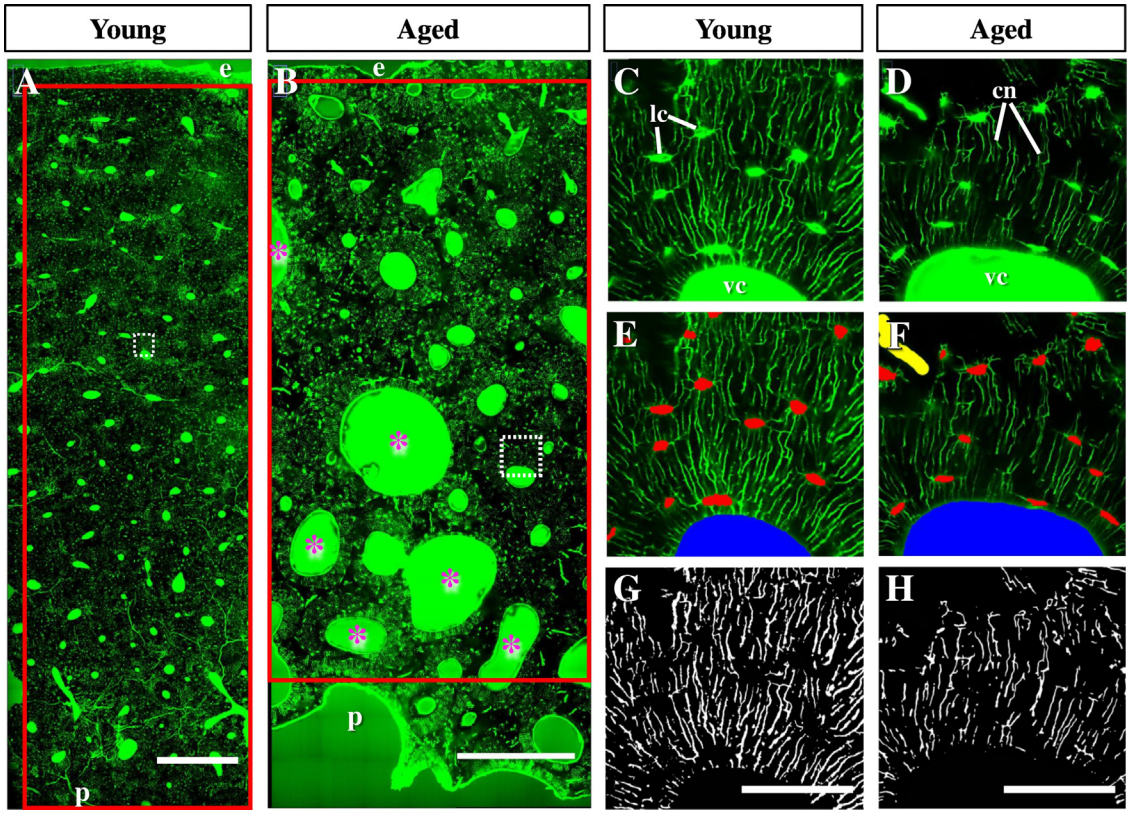

Fig. 1. Confocal imaging of femoral bone sections following FITC-labelling. A,B) Large montages that span the endosteal (e) to periosteal (p) edges of cortical bone from young (A; age 22) and aged (B; age 78) female donors. Red boxes outline the cropped image that was used for segmentation and analysis. White dashed boxes are regions expanded in C—H. Greater resorption spaces are clearly evident in the sample from the aged donor (B; a few examples are labelled with pink asterisks). C,D) Close-up of the cortical bone microarchitecture (white box in A,B) showing larger vascular canals (vc) in the sample from an aged donor, similarly sized lacunae (lc), and greater canalicular (cn) density in the sample from a young donor. E,F) Vascular canal (blue), artifacts (yellow), and lacunae (red) masks applied, leaving only the green fluorescence from the canaliculi. G,H) Vascular canals, artifacts, and lacunae were black-filled and remaining image was converted to binary allowing quantitation of canalicular porosity. Scale bar in (A,B) is 500 μm and in (G,H) is 50 μm. (For interpretation of the references to color in this figure legend, the reader is referred to the web version of this article.)

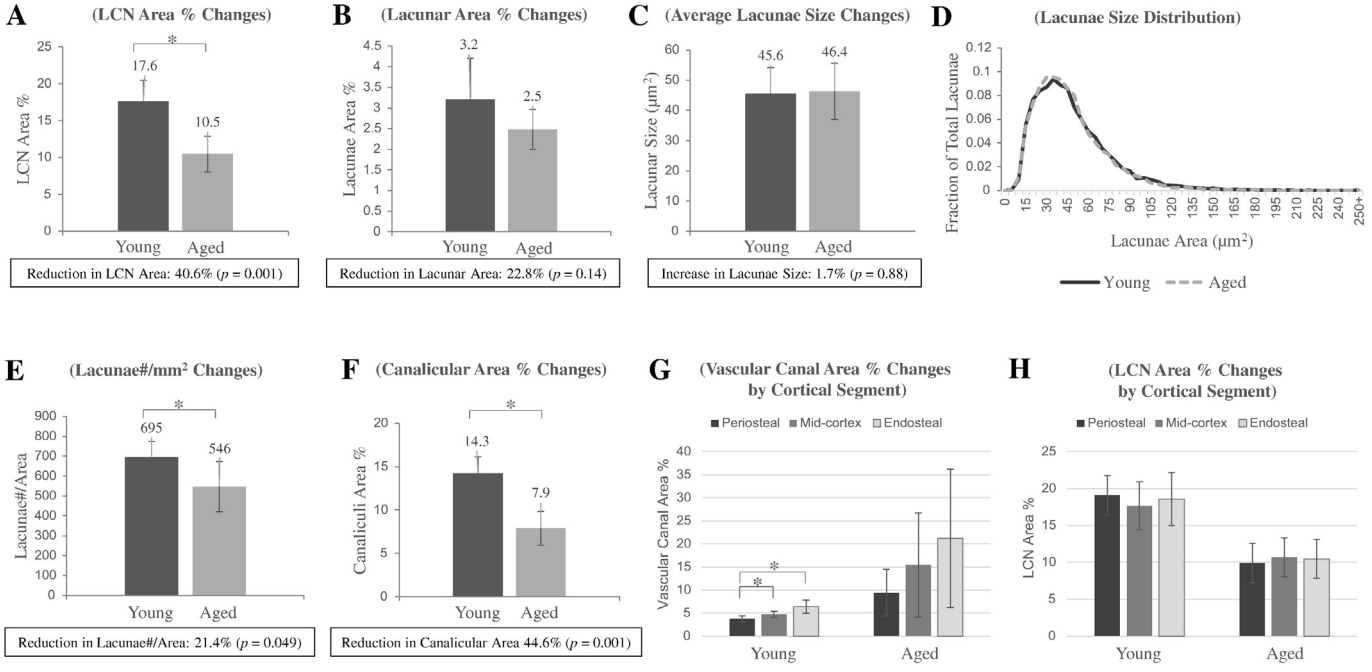

Fig. 2. Lacunar-canalicular and vascular canal characteristics of the femoral cortical bone in young and aged women. Inter-group differences in (A) LCN area percentage, (B) lacunar area percentage, (C) average lacunae size, (D) lacunae size distribution, (E) lacunae number per area (mm^2), (F) canalicular area percentage. Intra-cortical regional differences in (G) vascular canal and (H) LCN area percentages between the periosteal, mid-cortex, and endosteal regions. (* - $p < 0.05$). Error bars represent SD.

depth for confocal microscopy (0.44 μm). As such, an apparent decline in density observed in 2D can occur despite no change in 3D density. These discrepancies between 2D and 3D highlight methodological limitations facing LCN analysis. While 3D methods have a number of advantages, they often suffer from a reduced field of view. That said, our regional analysis suggests the scale of the LCN and its components are uniform across the cortex and thus sub-sampling smaller regions can generate a representative result with the caveat that considerable local variation in the LCN was observed in our images and thus sampling too small a region could lead to highly variable results. Similarly, spatial heterogeneity in canalicular density within osteons was recently reported (Repp et al., 2017). We believe that our observations that the LCN is uniform across the anterior femoral cortex and declines uniformly in aged women, are unique observations of this study. This stands in stark contrast to the regional differences observed in vascular canal porosity across the cortex which we detected here and others have reported (Thomas et al., 2005), indicating that the density of the LCN and its components is independent of vascular canal porosity. Potential circumferential variation of the LCN within the femoral cortex is worthy of further study as differences in the vascular canal porosity (Thomas et al., 2005) and the density and morphology of lacunae (Carter et al., 2013b) have been reported from other studies of Melbourne Femur Collection samples.

To summarise, we examined cortical bone from the anterior proximal femoral shaft and detected a significant reduction in the scale of the LCN in aged women compared to younger women. The lower LCN porosity in aged women could contribute to impaired intercellular communication between osteocytes because of fewer connections between these cells and thereby perturb their mechanosensation/mechanotransduction functions. Our observations warrant further research into the timing and mechanisms of these changes, and their possible role in bone loss associated with aging and osteoporosis.

Conflict of interest

All authors' declare that they have no conflicts of interest.

Author's roles

Project design: AMA, LSH, CDLT, JGC, PP, YC and DMLC. Experimentation and data collection: AMA, LSH, YC and DDM. Data analysis and interpretation: AMA, LSH, and DMLC. Drafting manuscript: AMA and LSH. Revising manuscript content and approving final version of manuscript: all authors. AMA and DMLC take responsibility for integrity of data analysis.

Acknowledgements

We are grateful to the mortuary staff and the staff of the Donor Tissue Bank of the Victorian Institute of Forensic Medicine for their assistance in the collection of this series of bone specimens, and we are particularly grateful to the next-of-kin of the donors for permission to remove bone for research purposes. We thank Dr. Jennifer Nyarko (the Cell Signalling Laboratory, Department of Psychiatry, University of Saskatchewan) for consultation on use of the confocal laser scanning microscope. Support for this research was provided by the Canadian Institutes of Health Research (CIHR RPP: RSN-132194) and the Saskatchewan Health Research Foundation (SHRF: 2890).

Appendix A. Supplementary data

Supplementary data to this article can be found online at http://dx.doi.org/10.1016/j.bonr.2017.06.002.

References

Atkinson, P.J., Hallsworth, A.S., 1983. The changing pore structure of aging human mandibular bone. Gerodontology 2 (2), 57–66.
Benalla, M., Palacio-Mancheno, P.E., Fritton, S.P., Cardoso, L., Cowin, S.C., 2014. Dynamic permeability of the lacunar-canalicular system in human cortical bone. Biomech. Model. Mechanobiol. 13 (4), 801–812.
Bonewald, L.F., 2007. Osteocytes as dynamic multifunctional cells. Ann. N. Y. Acad. Sci. 1116, 281–290.
Buenzli, P.R., Sims, N.A., 2015. Quantifying the osteocyte network in the human skeleton. Bone 75, 144–150.
Busse, B., Djonic, D., Milovanovic, P., Hahn, M., Puschel, K., Ritchie, R.O., Djuric, M., Amling, M., 2010. Decrease in the osteocyte lacunar density accompanied by hypermineralized lacunar occlusion reveals failure and delay of remodeling in aged human bone. Aging Cell 9 (6), 1065–1075.
Carter, Y., Thomas, C.D., Clement, J.G., Cooper, D.M., 2013a. Femoral osteocyte lacunar density, volume and morphology in women across the lifespan. J. Struct. Biol. 183 (3), 519–526.
Carter, Y., Thomas, C.D., Clement, J.G., Peele, A.G., Hannah, K., Cooper, D.M., 2013b. Variation in osteocyte lacunar morphology and density in the human femur—a synchrotron radiation micro-CT study. Bone 52 (1), 126–132.
Carter, Y., Suchorab, J.L., Thomas, C.D., Clement, J.G., Cooper, D.M., 2014. Normal variation in cortical osteocyte lacunar parameters in healthy young males. J. Anat. 225 (3), 328–336.
Ciani, C., Doty, S.B., Fritton, S.P., 2009. An effective histological staining process to visualize bone interstitial fluid space using confocal microscopy. Bone 44 (5), 1015–1017.
Clement, J.G., 2005. The Melbourne femur collection: the gift of tissue underpins important medical and forensic research. VIFM Rev. 3, 7–11.
Cowin, S.C., 1999. Bone poroelasticity. J. Biomech. 32 (3), 217–238.
Cowin, S.C., 2002. Mechanosensation and fluid transport in living bone. J. Musculoskelet. Neuronal Interact. 2 (3), 256–260.
Currey, J.D., 1964. Metabolic starvation as a factor in bone reconstruction. Acta Anat. (Basel) 59, 77–83.
Currey, J.D., Shahar, R., 2013. Cavities in the compact bone in tetrapods and fish and their effect on mechanical properties. J. Struct. Biol. 183 (2), 107–122.
Gardinier, J.D., Townend, C.W., Jen, K.P., Wu, Q., Duncan, R.L., Wang, L., 2010. In situ permeability measurement of the mammalian lacunar-canalicular system. Bone 46 (4), 1075–1081.
Goulet, G.C., Coombe, D., Martinuzzi, R.J., Zernicke, R.F., 2009. Poroelastic evaluation of fluid movement through the lacunocanalicular system. Ann. Biomed. Eng. 37 (7), 1390–1402.
Hennig, C., Thomas, C.D., Clement, J.G., Cooper, D.M., 2015. Does 3D orientation account for variation in osteon morphology assessed by 2D histology? J. Anat. 227 (4), 497–505.
Hesse, B., Langer, M., Varga, P., Pacureanu, A., Dong, P., Schrof, S., Mannicke, N., Suhonen, H., Olivier, C., Maurer, P., Kazakia, G.J., Raum, K., Peyrin, F., 2014a. Alterations of mass density and 3D osteocyte lacunar properties in bisphosphonate-related osteonecrotic human jaw bone, a synchrotron microCT study. PLoS One 9 (2), e88481.
Hesse, B., Mannicke, N., Pacureanu, A., Varga, P., Langer, M., Maurer, P., Peyrin, F., Raum, K., 2014b. Accessing osteocyte lacunar geometrical properties in human jaw bone on the submicron length scale using synchrotron radiation muCT. J. Microsc. 255 (3), 158–168.
Hesse, B., Varga, P., Langer, M., Pacureanu, A., Schrof, S., Mannicke, N., Suhonen, H., Maurer, P., Cloetens, P., Peyrin, F., Raum, K., 2015. Canalicular network morphology is the major determinant of the spatial distribution of mass density in human bone tissue: evidence by means of synchrotron radiation phase-contrast nano-CT. J. Bone Miner. Res. 30 (2), 346–356.
Hirose, S., Li, M., Kojima, T., de Freitas, P.H., Ubaidus, S., Oda, K., Saito, C., Amizuka, N., 2007. A histological assessment on the distribution of the osteocytic lacunar canalicular system using silver staining. J. Bone Miner. Metab. 25 (6), 374–382.
van Hove, R.P., Nolte, P.A., Vatsa, A., Semeins, C.M., Salmon, P.L., Smit, T.H., Klein-Nulend, J., 2009. Osteocyte morphology in human tibiae of different bone pathologies with different bone mineral density—is there a role for mechanosensing? Bone 45 (2), 321–329.
Jilka, R.L., O'Brien, C.A., 2016. The role of osteocytes in age-related bone loss. Curr. Osteoporos. Rep. 14 (1), 16–25.
Kameo, Y., Adachi, T., Sato, N., Hojo, M., 2010. Estimation of bone permeability considering the morphology of lacuno-canalicular porosity. J. Mech. Behav. Biomed. Mater. 3 (3), 240–248.
Kamioka, H., Honjo, T., Takano-Yamamoto, T., 2001. A three-dimensional distribution of osteocyte processes revealed by the combination of confocal laser scanning microscopy and differential interference contrast microscopy. Bone 28 (2), 145–149.
Knothe Tate, M.L., Tani, A.E.G., Bauer, T.W., Knothe, U., 2002. Micropathoanatomy of osteoporosis: indicators for a cellular basis of bone disease. Advances in Osteoporotic Fracture Management. 2, pp. 9–14.
Knothe Tate, M.L., Adamson, J.R., Tami, A.E., Bauer, T.W., 2004. The osteocyte. Int. J. Biochem. Cell Biol. 36 (1), 1–8.
Kogianni, G., Noble, B.S., 2007. The biology of osteocytes. Curr. Osteoporos. Rep. 5 (2), 81–86.
Milovanovic, P., Zimmermann, E.A., Hahn, M., Djonic, D., Puschel, K., Djuric, M., Amling, M., Busse, B., 2013. Osteocytic canalicular networks: morphological implications for altered mechanosensitivity. ACS Nano 7 (9), 7542–7551.
Mori, S., Harruff, R., Ambrosius, W., Burr, D.B., 1997. Trabecular bone volume and microdamage accumulation in the femoral heads of women with and without femoral neck fractures. Bone 21 (6), 521–526.

Mullender, M.G., Huiskes, R., Versleyen, H., Buma, P., 1996. Osteocyte density and histomorphometric parameters in cancellous bone of the proximal femur in five mammalian species. J. Orthop. Res. 14 (6), 972–979.
Mullender, M.G., Tan, S.D., Vico, L., Alexandre, C., Klein-Nulend, J., 2005. Differences in osteocyte density and bone histomorphometry between men and women and between healthy and osteoporotic subjects. Calcif. Tissue Int. 77 (5), 291–296.
Noble, B.S., Reeve, J., 2000. Osteocyte function, osteocyte death and bone fracture resistance. Mol. Cell. Endocrinol. 159 (1–2), 7–13.
Okada, S., Yoshida, S., Ashrafi, S.H., Schraufnagel, D.E., 2002. The canalicular structure of compact bone in the rat at different ages. Microsc. Microanal. 8 (2), 104–115.
Otsu, N., 1979. A threshold selection method from gray-level histograms. IEEE Trans. Syst. Man Cybern. 9, 62–66.
Palacio-Mancheno, P.E., Larriera, A.I., Doty, S.B., Cardoso, L., Fritton, S.P., 2014. 3D assessment of cortical bone porosity and tissue mineral density using high-resolution micro-CT: effects of resolution and threshold method. J. Bone Miner. Res. 29 (1), 142–150.
Palumbo, C., Palazzini, S., Marotti, G., 1990. Morphological study of intercellular junctions during osteocyte differentiation. Bone 11 (6), 401–406.
Preibisch, S., Saalfeld, S., Tomancak, P., 2009. Globally optimal stitching of tiled 3D microscopic image acquisitions. Bioinformatics 25 (11), 1463–1465.
Qiu, S., Rao, D.S., Palnitkar, S., Parfitt, A.M., 2002. Age and distance from the surface but not menopause reduce osteocyte density in human cancellous bone. Bone 31 (2), 313–318.
Qiu, S., Rao, D.S., Palnitkar, S., Parfitt, A.M., 2003. Reduced iliac cancellous osteocyte density in patients with osteoporotic vertebral fracture. J. Bone Miner. Res. 18 (9), 1657–1663.
Qiu, S., Rao, D.S., Palnitkar, S., Parfitt, A.M., 2006. Differences in osteocyte and lacunar density between Black and White American women. Bone 38 (1), 130–135.
Repp, F., Kollmannsberger, P., Roschger, A., Kerschnitzki, M., Berzlanovich, A., Gruber, G.M., Roschger, P., Wagermaier, W., Weinkamer, R., 2017. Spatial heterogeneity in the canalicular density of the osteocyte network in human osteons. Bone Rep. 6, 101–108.
Rodriguez-Florez, N., Oyen, M.L., Shefelbine, S.J., 2014. Age-related changes in mouse bone permeability. J. Biomech. 47 (5), 1110–1116.
Schneider, P., Meier, M., Wepf, R., Muller, R., 2010. Towards quantitative 3D imaging of the osteocyte lacuno-canalicular network. Bone 47 (5), 848–858.
Scheiner, S., Pivonka, P., Hellmich, C., 2016. Poromicromechanics reveals that physiological bone strains induce osteocyte-stimulating lacunar pressure. Biomech. Model. Mechanobiol. 15 (1), 9–28.
Seeman, E., 2002. Pathogenesis of bone fragility in women and men. Lancet 359 (9320), 1841–1850.
Shapiro, F., Cahill, C., Malatantis, G., Nayak, R.C., 1995. Transmission electron microscopic demonstration of vimentin in rat osteoblast and osteocyte cell bodies and processes using the immunogold technique. Anat. Rec. 241 (1), 39–48.
Sharma, D., Ciani, C., Marin, P.A., Levy, J.D., Doty, S.B., Fritton, S.P., 2012. Alterations in the osteocyte lacunar-canalicular microenvironment due to estrogen deficiency. Bone 51 (3), 488–497.
Soicher, M.A., Wang, X., Zauel, R.R., Fyhrie, D.P., 2011. Damage initiation sites in osteoporotic and normal human cancellous bone. Bone 48 (3), 663–666.
Thomas, C.D., Feik, S.A., Clement, J.G., 2005. Regional variation of intracortical porosity in the midshaft of the human femur: age and sex differences. J. Anat. 206 (2), 115–125.
Tommasini, S.M., Trinward, A., Acerbo, A.S., De Carlo, F., Miller, L.M., Judex, S., 2012. Changes in intracortical microporosities induced by pharmaceutical treatment of osteoporosis as detected by high resolution micro-CT. Bone 50 (3), 596–604.
Varga, P., Hesse, B., Langer, M., Schrof, S., Mannicke, N., Suhonen, H., Pacureanu, A., Pahr, D., Peyrin, F., Raum, K., 2015. Synchrotron X-ray phase nano-tomography-based analysis of the lacunar-canalicular network morphology and its relation to the strains experienced by osteocytes in situ as predicted by case-specific finite element analysis. Biomech. Model. Mechanobiol. 14 (2), 267–282.
Vashishth, D., Gibson, G.J., Fyhrie, D.P., 2005. Sexual dimorphism and age dependence of osteocyte lacunar density for human vertebral cancellous bone. Anat. Rec. A Discov. Mol. Cell. Evol. Biol. 282 (2), 157–162.
Vatsa, A., Breuls, R.G., Semeins, C.M., Salmon, P.L., Smit, T.H., Klein-Nulend, J., 2008. Osteocyte morphology in fibula and calvaria — is there a role for mechanosensing? Bone 43 (3), 452–458.
Weiner, S., Wagner, H.D., 1998. THE MATERIAL BONE: structure-mechanical function relations. Annu. Rev. Mater. Sci. 28, 271–298.